Investigation into Some Tribological Properties of Plasma Nitrided Hot-Worked Tool Steel AISI H11

B.S. Yilbas, A.Z. Sahin, S.A.M. Said, J. Nickel, and A. Coban

Interest in the tribological properties of plasma nitriding has increased substantially over the past years because plasma nitriding provides a high nitride depth and improved hard facing. The present study examines the tribological properties of AISI H11 plasma nitrided, hot-worked steel. Different nitriding temperatures and durations were considered. Characterization of the composite structures was investigated with wear tests, x-ray diffraction (XRD) analysis, scanning electron microscopy (SEM), and microhardness tests. The depth profile of the nitrided zone was measured using the nuclear reaction analysis (NRA) technique. Plasma nitriding affected the microhardness, wear properties, and morphology considerably. Increase in process temperature increased the nitride zone depth.

Keywords
plasma nitriding, tool steel, tribological properties

1. Introduction

TRIBOLOGICAL properties of material surfaces become important in a number of industrial applications where wear and corrosion are of concern. Material surface properties can be improved by various surface treatment techniques, including mechanical, thermal, physical, and chemical treatments. Ion implantation is a surface modification technique whereby ions of the dopant materials are generated, accelerated, and impacted into the target surface. Although the technique has been a standard manufacturing operation in the electronic industry for some time, it has only recently found commercial utility in other fields, such as metallurgy and mechanical manufacturing. Plasma nitriding improves catalytic performance, corrosion and oxidation resistance, adhesion, and surface mechanical properties (hardness, fatigue, friction, and wear resistance) (Ref 1). Improvements in wear resistance results are due to increase in the hardness and yield strength of the substrate and decrease in friction coefficient.

Hardness increases are due to pinning of dislocations, strain in the lattice due to the implanted element (formation of new phases), that is, nitrides (Ref 2).

Plasma and ion nitriding have a number of advantages over gas nitriding, especially in the treatment of stainless steels, which are generally considered difficult to nitride (Ref 3). At temperatures attained in plasma treatment, nitrided stainless steels retain well their hardness and corrosion resistance. Nitrogen implantation has been carried out in a large number of steels, other than stainless steel, such as plain carbon steel, tool steels, and low alloy steels (Ref 4). Improvement in wear behavior is significant for titanium alloys and ductile steels and very slight for hardened (martensitic) steels (Ref 5, 6). Nitrogen implantation also was reported to improve the wear resistance of already nitrided steels (Ref 7).

B.S. Yilbas, A.Z. Sahin, S.A.M. Said, J. Nickel, and A Coban, Department of Mechanical Engineering, King Fahd University of Petroleum and Minerals, Dhahran 31261, Saudi Arabia.

Hot-worked tool steels (AISI H11) are most commonly used in manufacturing as die materials and require improved tribological surface properties, which tolerate thermal and mechanical cycling during operations. The lifetimes of dies are limited by the friction and wear properties of the die material. Failures in friction properties of the contacting surface result in abrasive wear, causing the die to fail in a very short time, which in turn results in high production costs. Consequently, improvement in surface properties of hot-worked tool steels becomes essential.

The present study examines the plasma nitriding of AISI H11 hot-worked steel to improve tribological properties. Different nitriding temperatures and durations are considered. Wear behavior of the substrate was investigated under dry and lubricated conditions. Cross sections of samples after nitriding were examined using SEM. The depth profile of the nitrided zone was measured using NRA.

2. Experimental

2.1 *Workpiece*

AISI H11 hot-worked tool steel was obtained from a commercial source. Table 1 gives the elemental contents of the material. All the workpieces were machined in the form of disks with 45 mm diameter and 12 mm width. Samples were then polished to obtain a surface roughness, R_a, of 0.1 to 0.3 μm. Workpieces (AISI H11 hot-worked tool steel) were quenched at 1080 °C and tempered at 570 °C for 1 h.

2.2 *Plasma Nitriding*

Workpiece surfaces were lap polished and cleaned prior to plasma nitriding with successive rinses of acetone, trichloroethylene, and methanol. Cleaned samples were placed in a plasma nitriding unit. A gas composition of N_2/H_2 having a partial pressure ratio of 9 to 1 at 250 Pa total pressure was used.

Table 1 Chemical composition of AISI H11 hot-worked steel

Composition, wt%					
C	Si	Mn	Cr	Mo	V
0.36	1.0	0.4	5.25	1.35	0.45

The workpiece surface temperature in the nitriding unit was altered between 540 to 580 °C by adjusting the surface current density. Nitriding time was set between 16 to 320 ks. Bias voltage was varied from –300 to –700 V direct current. Note that nitrogen molecules require a high dissociation energy, and under typical conditions (vacuum limits, gas), nitrogen atmosphere contains oxygen, which makes nitrogen an unattractive nitriding gas. Therefore, a mixture of N_2/H_2 is largely preferred because of the hydrogen reductive properties (Ref 8). The hydrogen reducing action, both in the gaseous phase (oxygen contamination) and on the substrate, leads to a considerable increase in the nitriding rates and oxidation rates.

Hydrogen also increases the electron mean velocity and produces NH by reaction with vibrationally excited nitrogen molecules in plasmas (Ref 9). This NH species enhances the nitriding process.

2.3 *Wear Tests*

Rolling wear test equipment was used (Fig. 1). Before being tested, the samples were carefully cleaned and weighed on a microbalance. After the friction pairs were fixed on the wear tester, the nitrided sample disk (lower disk, test disk) was rotated while the counterface disk was held stationary. ET025 oil (Welch Vacuum Technology) was introduced to the friction zone by a small pump, and the frictional force was recorded continuously throughout the test. The specimen disk rotational speed was kept constant at 100 revolutions per minute, and the effective applied load was varied in the range of 50 to 300 N. At every 100 m of sliding distance, the weight loss was measured, and a new contact line of the stationary counterface disk was ensured by slightly rotating the disk. After being tested, the specimens were rinsed with hexane to remove the paraffin oil lubricant and then ultrasonically agitated in acetone to remove adhered wear debris.

2.4 *Nuclear Reaction Analysis Measurement*

NRA of nitrogen was carried out in a 10 cm reaction chamber using the $N^{15}(p,\alpha\gamma)C^{12}$ reactions. Proton beams were provided by the 3 MV Tandetron Accelerator (KFUPM Energy Research Laboratory, King Fahd University of Petroleum and

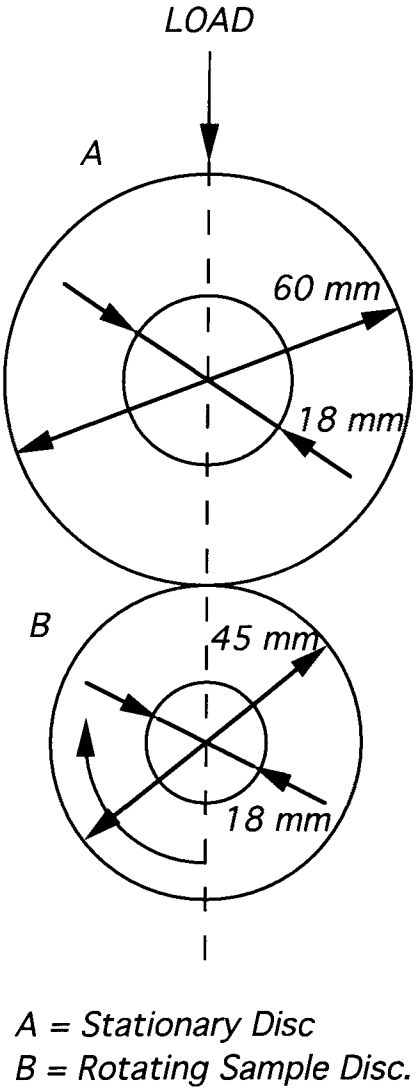

Fig. 1 Wear test configuration

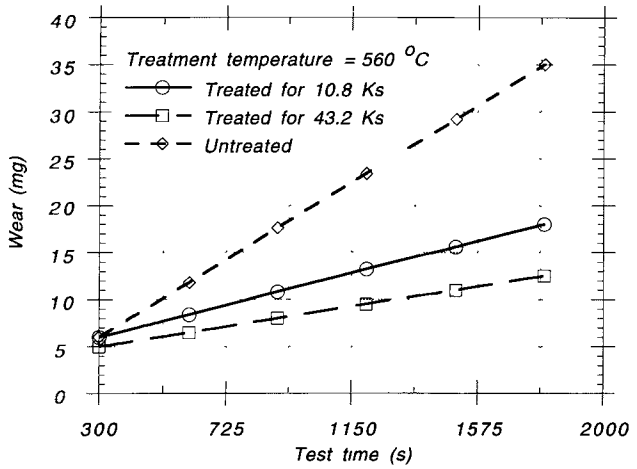

Fig. 2 Wear data with test duration

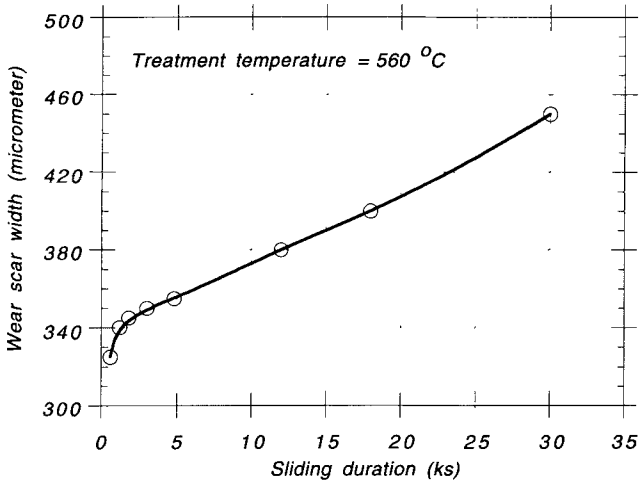

Fig. 3 Wear scar width with sliding time duration

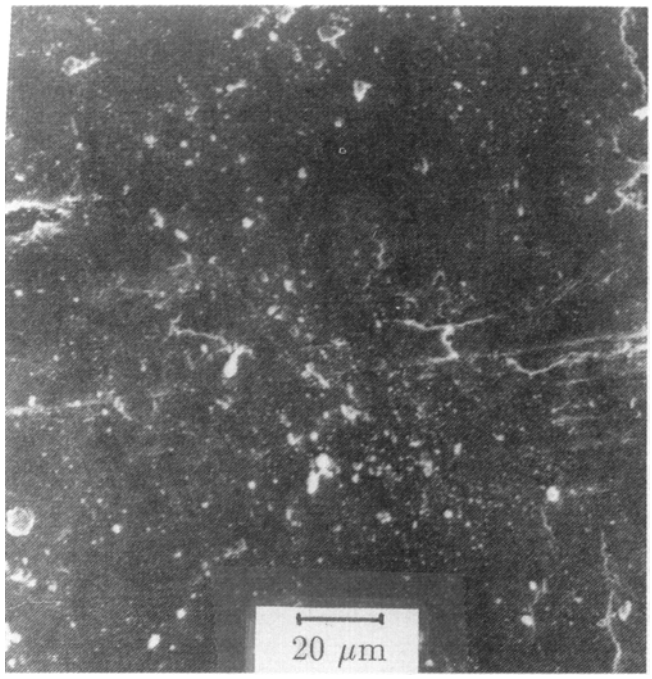

(a)

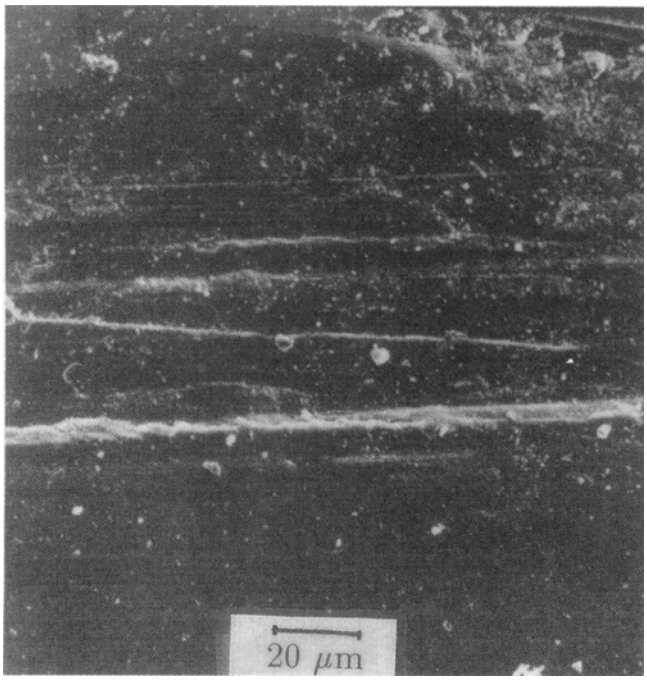

(b)

Fig. 4 Micrographs of wear surfaces after a test duration of (a) 5 ks and (b) 20 ks. Process temperature is 560 K, and process time is 320 ks.

Minerals, Saudi Arabia), and gamma rays were measured using a NaI(Tl) and/or a HpGe detector. The output of either detector was fed to standard NIM electronics (Nuclear Instruments Modules). The signals were processed by the VAX11/785 computer (Digital) using the on-line data acquisition code to produce the particle or γ-ray energy spectra. To minimize

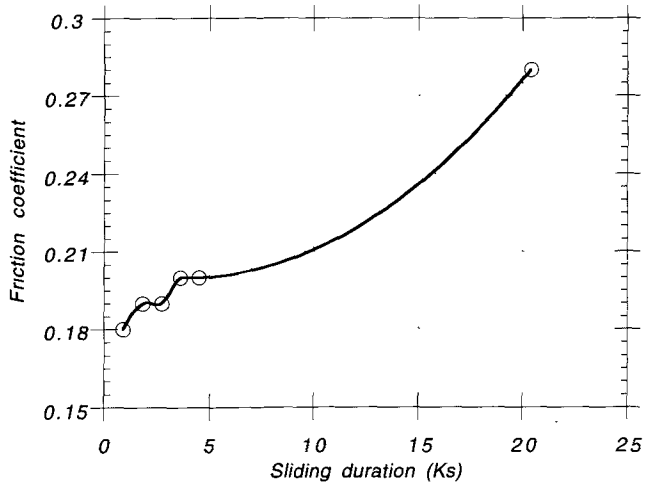

Fig. 5 Typical change of friction coefficient during the test as a function of time. Process temperature is 560 K. Nitriding time is 320 ks.

unwanted nuclear reactions in the chamber walls due to the scattered particles, the chamber walls were lined with a tantalum sheet. The chamber was electrically insulated from the rest of the beam line so that it could serve as a deep Faraday cup for beam-current measurements. Samples were manually positioned on a target ladder from outside without breaking the chamber vacuum. The beam was collimated on to the target using the three sets of slits in the beam line. To reduce carbon buildup on the target in the course of the experiments, a liquid nitrogen (LN_2) cooled 60-cm-long copper cold trap was put inside the beam line extending close to the sample.

2.5 *X-Ray Diffraction Analysis*

XRD analysis was carried out using Bragg-Bretone geometry with CuK_α radiation.

SEM was carried out to obtain micrographs of sample cross sections and surface damage due to wear tests.

3. Discussion

Figure 2 shows the wear data with test duration. Increased nitriding duration results in reduced wear, and long test duration evidently gives rise to poor wear resistance. Increasing nitriding duration results in homogeneously nitrided (clustered) matrix at the surface, which in turn increases the hardness and wear resistance consistent with the early work (Ref 8). During the initial test stage, the measured wear scar widths show a relatively small increase with increased sliding time. This initial wear stage, however, eventually triggers the next stage, in which the wear scar width rapidly increases with increasing sliding time (Fig. 3). After wear surface examination (Fig. 4), the wear surface is very smooth, but some fine scratches indicate the presence of abrasive wear in the sliding direction. Observations of the wear surface cross sections show that some part of the white layer is removed locally. The substrate begins to develop scars at the central region where the stress is higher. As the substrate is exposed, wear proceeds into the second

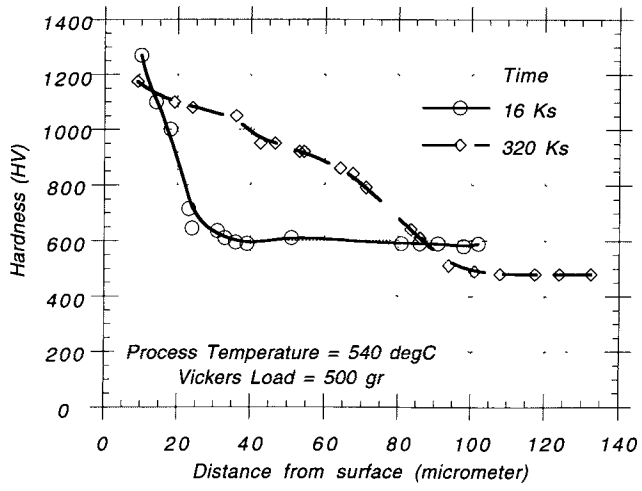

(a)

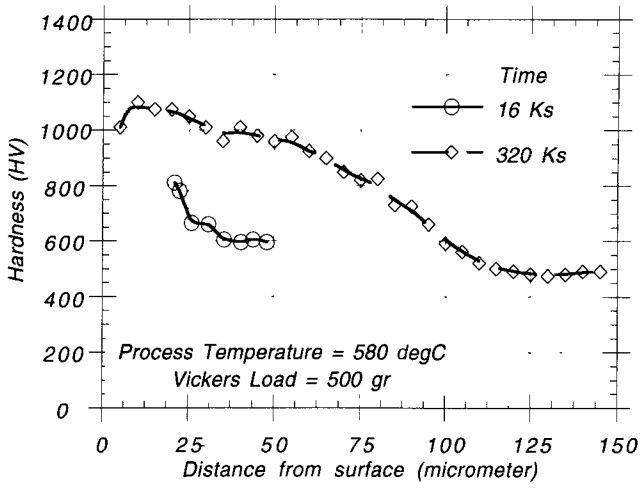

(b)

Fig. 6 Hardness test results for different combinations of nitriding parameters

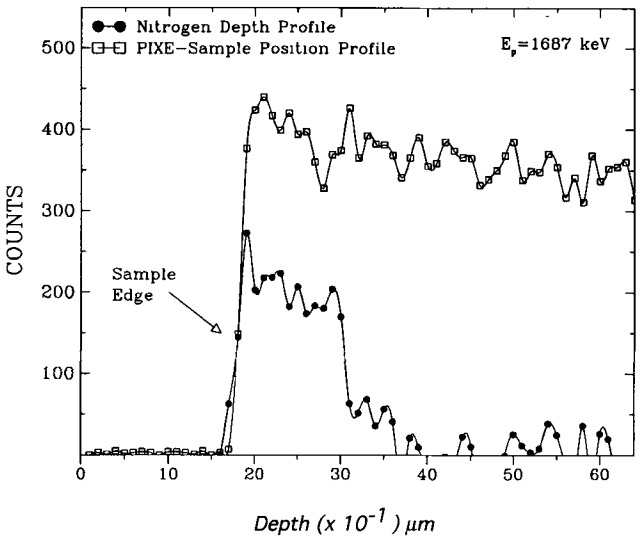

Fig. 7 Typical nuclear reaction analysis (NRA) measurement result for 320 ks nitriding duration and 540 °C process temperature

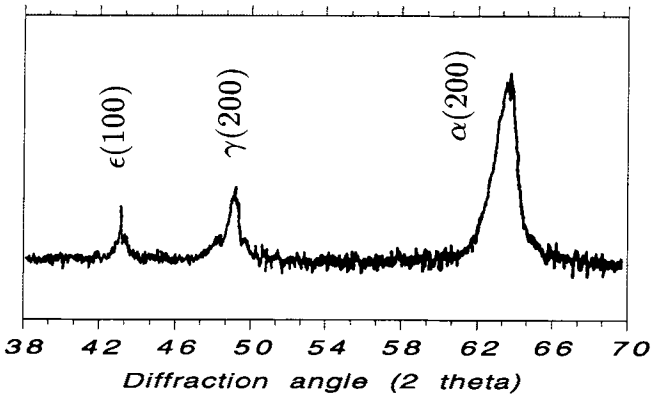

Fig. 8 X-ray diffractograms of the nitrided sample

Table 2 Physical and metallurgical data for AISI H11 before and after plasma nitriding

Material	Reflection plane (hkl)	Interplanar distance, nm	Lattice parameter, nm	Relative intensity, %	Compound layer
AISI H11	αFe(110)	0.2030	0.2862	76.9	...
	αFe(200)	0.1437	0.2874	56.7	...
Plasma nitrided AISI H11	αFe(110)	0.2060	0.2905	66.4	γ compound

stage. In this case, wearing develops rapidly, and mass removal rate increases considerably. Cho et al. (Ref 9) and Hockey (Ref 10) showed that severe damage resulting from plastic deformation accumulates in the substrate, which is subjected to sliding. The stress developed beneath the contacting asperities is sufficient to cause plastic deformation even in extremely brittle materials. However, the substrate tested has a hard nitride layer on a relatively soft substrate; therefore, extensive damage might be expected in the base material below the nitride zone.

Figure 5 shows the typical change of friction coefficient as a function of time. Friction coefficient varies slightly with sliding time for all the specimens. However, the friction coefficient increases rapidly once the transition in wear behavior occurs. This may be caused by the reduction in surface ductility due to nitride formation.

Figure 6 shows the hardness test results for different combinations of nitriding parameters. Hardness depth increases with increasing nitriding time. The nitride layer depth extends up to 100 μm. Hardness is highest in the surface region in which the compound layer developed. Compound layer increases with increasing nitriding time. A comparison of Fig. 6(a) and (b) shows the temperature effect. Nitriding depth increases slightly with increasing temperature. Note that alloy forming or chemically active species may enhance vacancy loop formation from

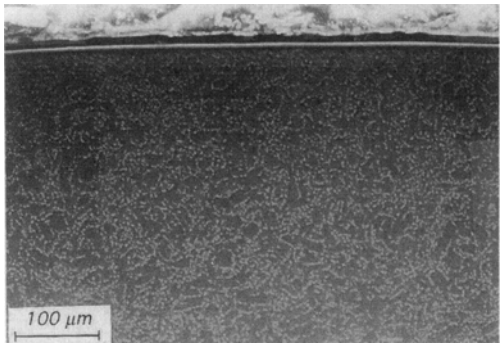

Fig. 9 Micrograph of nitrided sample cross section. Process time is 16 ks, and process temperature is 560 K.

vacancies generated in the displacement collision cascade (Ref 6), which in turn decreases slide dislocation mobility and increases hardness.

Figure 7 shows a typical NRA measurement result for 320 ks nitriding duration and 540 °C process temperature. This result agrees with the microhardness test results. Table 2 and Fig. 8 show the results of XRD analysis. CuK_α radiation was used as an x-ray source in a diffractometer. This part of the spectrum contains both αFe(110) and αFe(200) peaks from the sample. The plasma nitriding effect is clearly visible due to changes in shape and peak intensity of the αFe(110) diffraction line by viewing the diffractograms in Fig. 8. The asymmetry of the αFe(110) peaks is due to the variation in nitrogen level in the nitride diffusion zone of the layer, which gives a range of d-spacings. The lattice parameter and interplanar distance (Table 2) calculated from the αFe(110) peaks increase because of plasma nitriding of the substrate. The changes in the diffraction peak profiles and the lattice parameters after plasma nitriding of the substrate are due to the microstrains in the surface layer.

Figure 9 shows micrographs of nitrided sample cross sections. The compound layer thickness is ~10 μm. The compound layer consists of a monophase γ′ compound, which in turn enhances the layer properties. Almost homogeneous precipitation in nitrided zone occurs providing that the nitriding front advances parallel to the sample free surface.

4. Conclusions

The present work shows:

- Increase in nitriding time reduces wear. After the initial stage of the wear test, triggering of abrasive wear occurs, which in turn results in the next stage wearing. In this case, friction coefficient and width of the scars increases. Scratches indicate the presence of abrasive wear in the sliding direction.
- Friction coefficient stays almost constant in the first phase of wear; however, once the second phase is triggered, it increases abruptly.
- NRA study and microhardness test results show that nitride zone depth increases with nitriding time and process temperature. Increase in hardness may be due to pinning effect, or chemically active species may enhance vacancy loop formation from vacancies generated in the displacement collision cascade, which in turn decreases glide dislocation mobility and increasing hardness.
- Monophase γ′ compound layer occurs in the surface. Thickness of this layer varies with nitriding time and process temperature; i.e., increase in nitriding time and process temperature results in increase in compound layer thickness.
- A microphotograph of nitride zone cross sections shows that almost homogeneous precipitation occurs, and nitriding front advances parallel to the free surface of the samples in the neighborhood of compound layer.

Acknowledgment

The authors acknowledge the support of the Energy Research Laboratory of the Research Institute and the ME department of King Fahd University of Petroleum and Minerals, Dhahran, Saudi Arabia, for this work.

References

1. H. Kuwahara, H. Matsuoka, J. Takada, S. Kikuchi, Y. Tomii, and I. Tamura, Plasma Nitriding of Fe-18Cr-9N in the Range of 723-823 K, *Oxid. Met.*, Vol 36 (No. 1/2), 1991, p 143-156
2. M.M. Ibrahim, F.M. El-Hossary, N.Z. Negm, and M. Abed, Effect of RF Plasma Nitriding Time on Microhardness and Corrosion Resistance of 304 Stainless Steel, *Appl. Surf. Sci.*, Vol 59, 1992, p 253-260
3. M.M. Gopal, K.J. Vinod, M.U. Heidi, and D.B. Barrie, Effect of Ion Implantation on Friction and Wear Behaviour of Steels, *Wear*, Vol 159, 1992, p 47-55
4. W. Rembges and W. Oppel, Process Control of Plasma Nitriding and Plasma Nitrocarburizing in Industry, *Surf. Coat. Technol.*, Vol 59, 1993, p 129-134
5. F.E. Kennedy and L. Tang, Factors Affecting the Sliding Performance of Titanium Nitride Coating, *Mechanics of Coatings*, Elsevier, Amsterdam, 1989
6. P.D. Geode, Wear Mechanisms in Ferrous Alloys, *Nucl. Instrum. Methods Phys., Res. B*, Vol 39, 1989, p 521-525
7. C.A. Straede, Practical Applications of Ion Implantation for Tribological Modification of Surface, *Wear*, Vol 130, 1989, p 113-117
8. A. Szasz, D.J. Fabion, A. Hendry, and Z. Szaszne-Csih, Nitriding of Stainless Steel in RF Plasma, *J. Appl. Phys.*, Vol 66 (No. 11), 1989, p 5598-5601
9. S.J. Cho, B.J.H. Moon, and S.M. Hsu, The Transition from Mild to Severe Wear in Alumina during Sliding, *Acta Metall. Mater.*, Vol 40, 1992, p 185-192
10. B.J. Hockey, Plastic Deformation of Aluminium Oxide by Indentation and Abrasion, *J. Am. Ceram. Soc.*, Vol 54, 1971, p 223-231